

# Total Dose Tolerance of Monolithic Millimeter-Wave Transceiver Building Blocks Implemented in 200 GHz SiGe Technology

Wei-Min Lance Kuo, Yuan Lu, Brian Floyd, Becca M. Haugerud, Akil K. Sutton, Ramkumar Krithivasan  
John D. Cressler, Brian P. Gaucher, Paul W. Marshall, Robert A. Reed, and Greg Freeman

**Abstract**—This paper presents the first experimental results on the effects of 63.3 MeV proton irradiation on 60 GHz monolithic point-to-point broadband space data link transceiver building blocks implemented in a 200 SiGe HBT technology. A SiGe low-noise amplifier and a SiGe voltage-controlled oscillator were each irradiated to proton fluences of  $5.0 \times 10^{13}$  p/cm<sup>2</sup>. The device- and circuit-level performance degradation associated with these extreme proton fluences is found to be minimal, suggesting that such SiGe HBT transceivers should be robust for space applications, without intentional hardening at either the device or circuit level.

TABLE I  
SUMMARY OF THE SiGe HBT PARAMETERS

$W_E$	0.12 $\mu\text{m}$
Peak $\beta$	400
Peak $f_T$	207 GHz
Peak $f_{max}$	285 GHz
$BV_{CEO}$	1.7 V
$BV_{CBO}$	5.5 V

## I. INTRODUCTION

An important emerging market for millimeter-wave (mm-wave = > 30 GHz) IC technologies lies in very high bandwidth (> 1 Gb/sec) point-to-point communications data links [1][2]. Traditionally, discrete microwave integrated circuits implemented in III-V technologies (GaAs and/or InP) have been combined to realize mm-wave transceiver modules because they offered significant performance advantages at mm-wave frequencies over Si technologies. [3]-[5]. Unfortunately, such transceiver modules are typically power hungry, large, heavy and hence costly [6][7]. Clearly, for space applications of such mm-wave data links, achieving low power, small size, light weight, and low cost are essential requirements in addition to maintaining acceptable performance and high reliability. As will be demonstrated, an alternative IC technology based on silicon-germanium (SiGe) alloys can directly fulfill these requirements [8].

SiGe heterojunction bipolar transistor (HBT) technology utilizes bandgap engineering techniques to dramatically improve transistor-level performance while simultaneously maintaining strict compatibility with conventional silicon (Si) manufacturing [9]. The evolution of SiGe technology remarkably rapidly, and has today reached a point where SiGe HBT technology is of comparable performance with the best-of-breed III-V technologies. With the recent announcement of third-generation SiGe HBTs having peak cutoff frequency ( $f_T$ ) above 200 GHz [10] and fourth-generation technology having peak  $f_T$  above 300

GHz [11], the application space for SiGe HBT technology has further broadened from a variety of analog and radio frequency (RF) applications to now include monolithically integrated mm-wave communications systems. SiGe HBT technology thus combines III-V like device performance with the high integration, high yield, and hence low cost associated with Si to facilitate system-on-a-chip solutions. In addition, SiGe HBTs have also been shown to be robust with respect to total dose irradiation without any additional costly radiation hardening. With these attributes, SiGe HBT technology promises to provide high performance, high reliability, small size, light weight, and low cost required for monolithic mm-wave transceivers for space link applications.

This paper presents, for the first time, experimental results on the effects of proton irradiation on critical building blocks for such a 60 GHz monolithic mm-wave transceiver implemented in IBM's third-generation 200 GHz SiGe HBT technology.

## II. PROCESS TECHNOLOGY

The SiGe HBT technology investigated in this paper is the IBM SiGe 8T technology with 200 GHz peak  $f_T$  and 285 peak maximum oscillation frequency ( $f_{max}$ ) [10]. It features copper interconnects with a thick top layer aluminum metallization and a full suite of passive elements. This advance in the SiGe state-of-the-art to 200 GHz transistor performance was only achieved by radically altering the structure of previous SiGe HBT design points. The present technology employs a novel, reduced thermal cycle, "raised extrinsic base" structure, and utilizes conventional deep and shallow trench isolation, an *in-situ* doped polysilicon emitter, and an unconditionally stable, 25% peak Ge, C-doped, graded UHV/CVD epitaxial SiGe base. The device structure has been scaled laterally to 0.12  $\mu\text{m}$  emitter stripe width in order to minimize base resistance and thus improve the frequency response and noise characteristics. Such a raised extrinsic base structure facilitates the elimination of any out-diffusion of the extrinsic base, thereby significantly lowering the collector-base

This work was supported by NASA Glenn (contract # NAS3-03070), DTRA under the Radiation Tolerant Microelectronics Program, NASA-GSFC under the Electronics Radiation Characterization Program, IBM, and the Georgia Electronic Design Center at Georgia Tech.

W.-M.L. Kuo, Y. Lu, B.M. Haugerud, A.K. Sutton, R. Krithivasan, and J.D. Cressler are with the School of Electrical and Computer Engineering, 85 Fifth Street, N.W., Georgia Institute of Technology, Atlanta, GA 30332-0250, USA. Tel: (404) 894-5161 / Fax: (404) 894-4641 / E-mail: kuolance@ece.gatech.edu

B. Floyd and B. Gaucher are with the IBM Research Division, Thomas J. Watson Research Center, Yorktown Heights, NY 10598 USA.

P.W. Marshall is a consultant to NASA-GSFC.

R.A. Reed is with NASA-GSFC, Greenbelt, MD 20771 USA.

G. Freeman is with IBM, Hopewell Junction, NY 12533 USA.

junction capacitance. This SiGe HBT technology has not been intentionally radiation-hardened in any way. Typical transistor parameters are summarized in Table I.

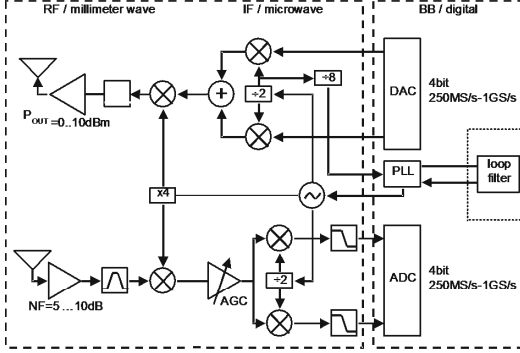


Fig. 1. A 60 GHz mm-wave space communications transceiver block diagram (after [8]).

### III. EXPERIMENT

The goal of this work was to carefully assess the impact of radiation exposure on actual 60 GHz monolithic mm-wave transceiver building blocks implemented in 200 GHz SiGe HBT technology, and use an additional transistor-level radiation experiment to better understand the observed circuit response. A 60 GHz mm-wave transceiver block diagram is shown in Figure 1. Two key components are chosen for this study: one is the low-noise amplifier (LNA), which is used to amplify the received signals while adding minimal noise; the other is the voltage-controlled oscillator (VCO), which is used to generate local oscillator (LO) signals for up- and down-conversion mixers. Each SiGe circuit was designed, laid out, fabricated, and characterized before and after being irradiated, along with SiGe HBT *dc* and *ac* test structures needed for correlating changes in circuit performances back to device parameters.

The samples were irradiated with 63.3 MeV protons at the Crocker Nuclear Laboratory at the University of California at Davis. The dosimetry measurements used a five-foil secondary emission monitor calibrated against a Faraday cup. Ta scattering foils located several meters upstream of the target establish a beam spatial uniformity of 15% over a 2.0 cm radius circular area. Beam currents from about 20 nA to 100 nA allow testing with proton fluxes from  $1.0 \times 10^9$  to  $1.0 \times 10^{12}$  proton/cm<sup>2</sup>sec. The dosimetry system has been previously described [12][13], and is accurate to about 10%. At proton fluences of  $1.0 \times 10^{12}$  and  $5.0 \times 10^{13}$  p/cm<sup>2</sup>, the measured equivalent gamma dose was approximately 135 and 6,759 krad (Si), respectively. The SiGe HBT *dc* test structures were irradiated with all terminals grounded, while the *ac* test structures and circuits were irradiated with all terminals floating. Previous studies have shown that this has minimal effect on the transistor-level radiation response [14]. All samples were irradiated to a proton fluence of  $5.0 \times 10^{13}$  p/cm<sup>2</sup>, while the *ac* test structures were re-irradiated with another proton fluence of  $5.0 \times 10^{13}$  p/cm<sup>2</sup> resulting in a net fluence of  $1.0 \times 10^{14}$  p/cm<sup>2</sup>.

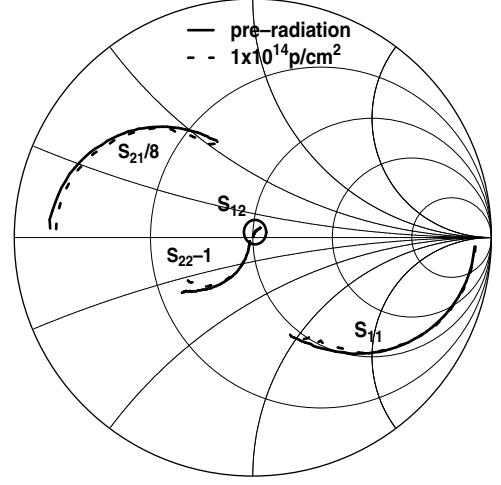


Fig. 2. Deembedded S-parameters at peak  $f_T$ .

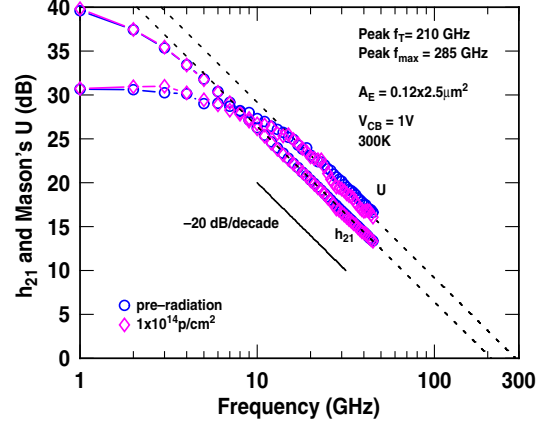


Fig. 3. Measured  $h_{21}$  and Mason's  $U$  versus frequency at peak  $f_T$ .

### IV. TRANSISTOR-LEVEL RESPONSE

Measurements of the SiGe HBT *dc* and *ac* test structures were made to quantify the transistor-level radiation response. Proton tolerance of a pre-production third-generation SiGe HBT technology has previously been reported in [15]. The SiGe HBTs used in this investigation represent an improved version of the one examined in [15], this time with an optimized ideal base current, reduced base resistance, and improved noise performance. The *dc* results obtained were in close agreement with the ones reported in [15] and, for brevity, are not repeated here.

The transistor scattering-parameters (S-parameters) were measured from 1 to 45 GHz at each bias point and subsequently deembedded using an "open-short" method. The current gain ( $h_{21}$ ), Mason's unilateral gain ( $U$ ), and base resistance ( $r_b$ ) were then calculated from the deembedded S-parameters. The  $f_T$  and  $f_{max}$  were extrapolated from  $h_{21}$  and Mason's  $U$  with a -20 dB/decade slope line to 0 dB. Typical pre- and post-radiation deembedded S-parameters biased at peak  $f_T$  are shown in Figure 2, the associated  $h_{21}$  and Mason's  $U$  are shown in Figure 3, and the extracted  $r_b$  is shown in Figure 4. The extrapolated  $f_T$  and  $f_{max}$  up to  $1.0 \times 10^{14}$  p/cm<sup>2</sup> proton fluenced are shown in Figure 5. Among the figures, the most apparent proton-induced device degradation lies in the increase of  $r_b$  in Figure 4, presumably

caused by displacement effects in the neutral base region and the deactivation of boron dopants. Clearly, these third-generation SiGe HBTs are remarkably total-dose hard at the transistor level without any intentional hardening.

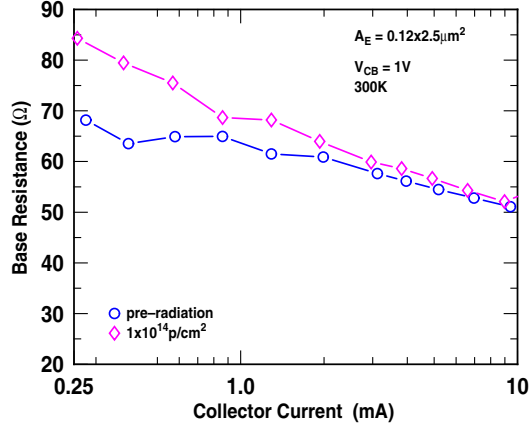


Fig. 4. Extracted base resistance ( $r_b$ ) versus collector current.

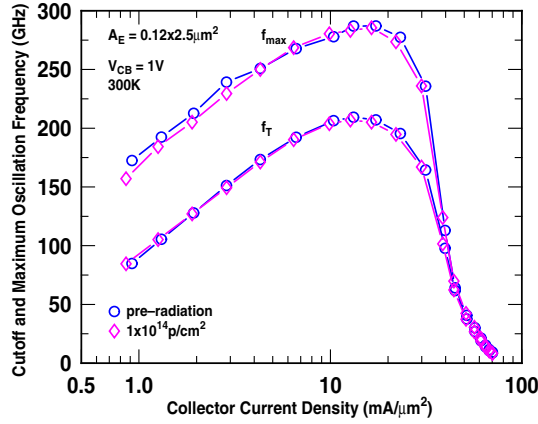


Fig. 5. Extrapolated  $f_T$  and  $f_{max}$  versus collector current density.

## V. LOW-NOISE AMPLIFIER

The LNA is a crucial building block in the SiGe monolithic mm-wave transceiver since it is the first gain stage in the receiver path used to amplify the weak incoming signals from the antenna. The noise figure ( $NF$ ) of the LNA adds directly to that of the overall transceiver [16]. Thus, gain and  $NF$  are two key metrics, along with the input impedance match ( $S_{11}$ ) and the output impedance match ( $S_{22}$ ) [9].

The 60 GHz SiGe LNA, whose schematic is shown in Figure 6a, employs a two-stage architecture using microstrip inductors. The gain is adjustable by changing the second-stage bias current. The LNA die micrograph is shown in Figure 6b, and the LNA occupies an area of  $0.92 \times 0.57 \text{ mm}^2$ . The pre- and post-radiation LNA gain and  $NF$  are shown in Figure 7 and 8, respectively. The LNA gain decreased by 0.5 dB,  $NF$  increased by 0.4 dB,  $S_{11}$  remained unchanged, and  $S_{22}$  increased by 1.5 dB. Detailed results are summarized in Table II. The results are robust and repeatable.

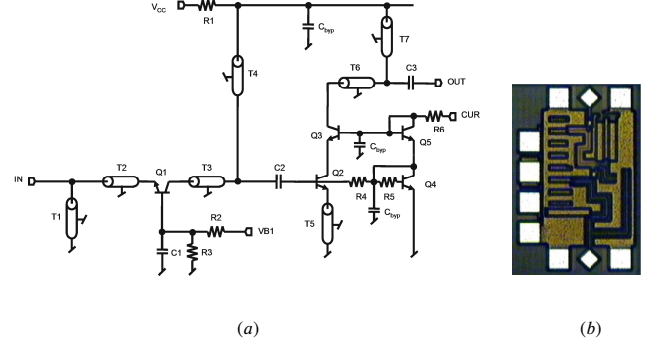


Fig. 6. The SiGe LNA: (a) schematic, and (b) die micrograph.

The proton-induced changes in the SiGe LNA performance are minor, proving that it is robust from a total dose perspective for space applications. The increase in  $S_{22}$  can be attributed to the effects of proton irradiation on the microstrip inductors, thereby changing the output matching point, which in turn degrades the gain. The increase in  $NF$  can be attributed to the increase in  $r_b$  (Figure 4) of the SiGe HBT, which adds directly to the  $NF$  of the LNA [9]. More detailed characterization of the proton-induced changes on the microstrip inductors is needed to accurately quantify their effects on the LNA at mm-wave frequencies, and is in progress.

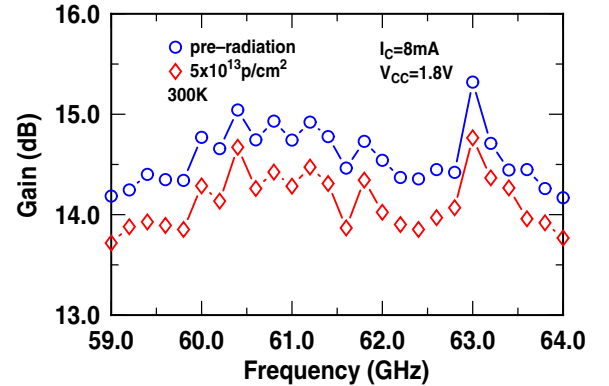


Fig. 7. Measured pre- and post-radiation gain of the SiGe LNA.

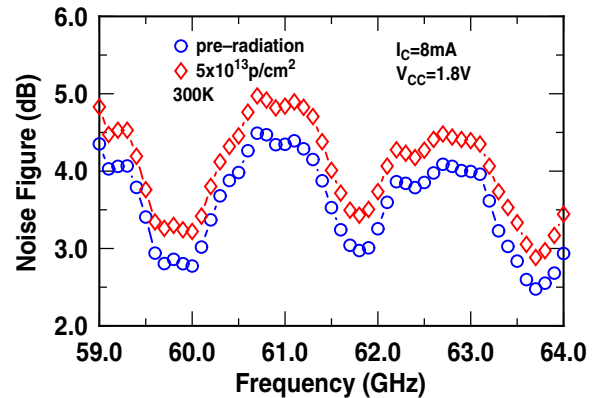


Fig. 8. Measured pre- and post-radiation noise figure of the SiGe LNA.

TABLE II  
SUMMARY OF THE SiGe TRANSCEIVER BUILDING BLOCK PARAMETERS

Block	Parameters	Pre-radiation	Post-radiation	Units
LNA	Frequency	61.5	61.5	GHz
	Gain	14.5	14.0	dB
	$NF$	3.6	4.0	dB
	$S_{11}$	-6.0	-6.0	dB
	$S_{22}$	-18.0	-16.5	dB
	$V_{cc}$	1.8	1.8	V
	$I_c$	8	8	mA
VCO	Frequency	67.3	67.5	GHz
	$P_{out}$	-11	-11	dBm
	$L(1 \text{ MHz})$	-102	-100	dBc/Hz
	$V_{cc}$	3	3	V
	$I_c$	8	8	mA

## VI. VOLTAGE-CONTROLLED OSCILLATOR

The VCO is another vital building block in the SiGe monolithic mm-wave transceiver. It is used to generate the local oscillator (LO) signals for the up- and down-conversion mixers needed to achieve frequency translation. Thus, the operating frequency of the VCO is a key performance parameter. The spectral purity of the VCO output is also key and is characterized by the phase noise. Phase noise can cause reciprocal mixing in the receiver and corrupt the wanted signal in the transmitter [16], both of which are detrimental to proper transceiver functionality.

The SiGe VCO, whose schematic is shown in Figure 9a, employs a differential Colpitts architecture with microstrip inductors and base-collector junction varactors. The VCO die micrograph is shown in Figure 9b, and the die occupies an area of  $0.9 \times 0.6 \text{ mm}^2$ . The pre- and post-radiation VCO power spectrum are essentially identical and thus, for brevity, only the post-radiation spectrum is shown in Figure 10. The VCO operating frequency shifted 0.2 GHz while the phase noise degraded 2 dB at 1 MHz offset when the varactor is biased at half of the supply voltage. Detailed results are summarized in Table II.

The proton-induced changes in the SiGe VCO performance are minor, proving that it is robust from a total dose perspective for space applications. The shift in operating frequency may be attributed to the effects of proton irradiation on the microstrip inductors and base-collector varactors that form the tank of the VCO. The degradation in phase noise may be attributed to an increase in SiGe HBT low-frequency noise ( $1/f$ ) noise [17] that is up-converted into phase noise. Similar observations were made in [14], but in that case on a 5 GHz VCO using first-generation SiGe HBT technology. More detailed characterization of the proton-induced changes on the microstrip inductors, base-collector varactors, and SiGe HBT  $1/f$  noise are needed to accurately quantify their effects on the VCO at mm-wave frequencies, and are in progress.

## VII. SUMMARY

The effects of 63.3 MeV proton irradiation on 60 GHz monolithic mm-wave transceiver building blocks implemented in third-generation SiGe HBT technology have been investigated

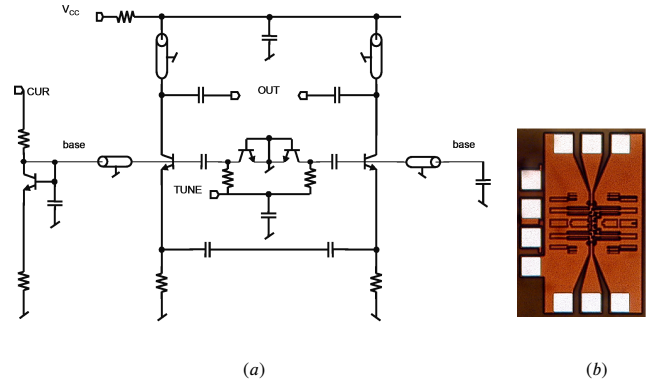


Fig. 9. The SiGe VCO: (a) schematic, and (b) die micrograph.

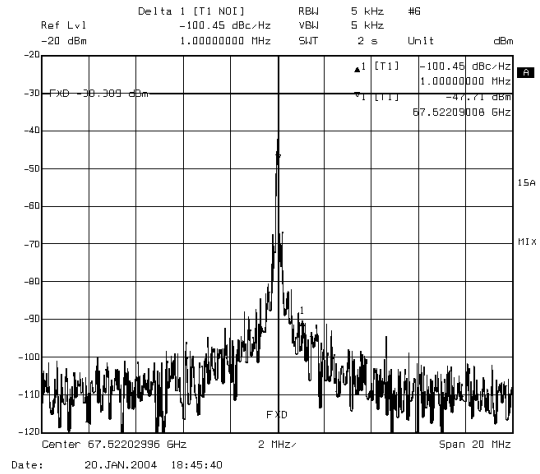


Fig. 10. The measured power spectrum of the post-irradiated SiGe VCO.

for the first time. A SiGe HBT 60 GHz LNA and VCO were irradiated to proton fluences of  $5.0 \times 10^{13} \text{ p/cm}^2$ . The degradation associated with these extreme proton fluences is found to be minor, suggesting that mm-wave SiGe transceiver building blocks should be robust to total ionizing dose for space applications.

## VIII. ACKNOWLEDGEMENT

The authors are grateful to J. Warner, L. Cohn, K. LaBel, T. Beukema, S. Reynolds, T. Zwick, U. Pfeiffer, D. Liu, M. Oprysko, A. Joseph, D. Harame, D. Ahlgren, D. Herman, B. Meyerson, and the IBM SiGe team for their contributions.

## REFERENCES

- [1] T. Takagi *et al.*, *IEEE Trans. MTT*, 49, p. 2073, 2001.
- [2] M. Soulard *et al.*, *Proc. ICMET*, p. 219, 2000.
- [3] C. Drevon, *IEEE Sem. Pack. Int. Micro. mm-Wave Freq.*, p. 8/1, 2000.
- [4] A. K. Oki *et al.*, *Proc. IEEE IPRM*, p. 7, 2000.
- [5] D. Streit *et al.*, *IEEE EDMO Symp. Tech. Dig.*, p. 14, 2002.
- [6] D. Yamauchi *et al.*, *IEEE IMS Tech. Dig.*, p. 2015, 2003.
- [7] M. Kärkkäinen *et al.*, *IEEE IMS Tech. Dig.*, p. 1273, 2002.
- [8] B. Gaucher *et al.*, *Proc. SMC-IT*, p. 113, 2003.
- [9] J.D. Cressler and G. Niu, *SiGe HBTs*, Artech House, MA, 2003.
- [10] B. Jagannathan *et al.*, *IEEE Elect. Dev. Lett.*, 23, p. 258, 2002.
- [11] J.-S. Rieh *et al.*, *IEEE IEDM Tech. Dig.*, p. 771, 2002.
- [12] K.M. Murray *et al.*, *Nucl. Inst. Meth.*, B56/57, p. 616, 1991.
- [13] P.W. Marshall *et al.*, *IEEE Trans. Nucl. Sci.*, 41, p. 1958, 1994.
- [14] J.D. Cressler *et al.*, *IEEE Trans. Nucl. Sci.*, 48, p. 2238, 2001.
- [15] Y. Lu *et al.*, *IEEE NSREC*, paper A-6, 2003.
- [16] B. Razavi, *RF Microelectronics*, Prentice Hall, NJ, 1998.
- [17] Z. Jin *et al.*, *IEEE Trans. Nucl. Sci.*, 48, p. 2244, 2001.